

Research Article

Research on Shape Feature Recognition of B-Rep Model Based on Wavelet Transform

Jihua Wang 

College of Information Science and Engineering, Shandong Normal University, No. 88 Wenhua East Road, Jinan 250014, China

Correspondence should be addressed to Jihua Wang; jihuaaw@126.com

Received 11 January 2018; Accepted 12 July 2018; Published 19 July 2018

Academic Editor: Erik Cuevas

Copyright © 2018 Jihua Wang. This is an open access article distributed under the Creative Commons Attribution License, which permits unrestricted use, distribution, and reproduction in any medium, provided the original work is properly cited.

B-Rep (Boundary Representation) CAD model is widely used in the representation of manufactured product in computer, and it is a kind of real 3D structure with invisible part relative to 2.5D mesh model, so the shape feature recognition of B-Rep model is worth of much studying. We present one approach of shape feature recognition of B-Rep model based on the wavelet transform of surface boundary and region; it is inspired by the neuropsychology view that surface is the key visual features and by the systematology method that an object is recognized by decomposing and grouping its similar parts. Surface elements of B-Rep model are extracted from the neutral STEP (Standard for Exchange of Product Model Data) file; the curvatures of surface boundary and region were decomposed by wavelet transform, and then the coefficient statistics of same scale were as the surface feature vector. Similar surfaces of B-Rep model were clustered as a bin with the sum of perimeters and the mean vector, and all bins constituting a histogram are finally as the feature vector of B-Rep model. Thus B-Rep models are compared and retrieved using the EMD (Earth Mover's Distance) of histogram. Our approach was evaluated by retrieval experiment with NDR (National Design Reservoir), and the result indicated its highly competent performance.

1. Introduction

Shape feature recognition of CAD model lays the solid foundation for content-based model retrieval, functions and structures mapping, design intent analysis throughout industrial product design, and manufacture field. B-Rep model is almost only representation way of CAD model related to manufactured objects, which is widely shared and exchanged in STEP format. Comparing with the mesh model as 2.5D model that only gives us overall visible appearance, B-Rep model as real 3D model has unambiguous internal schemes and contains rich design semantics such as geometric and topology variables, and it can be precisely expressed in the form of attributed adjacency graph (AAG) [1, 2]. B-Rep model shows its structures and characteristics by mathematical language in computer, but it does not directly provide us with recognition features. Therefore it is meaningful to extract the shape features of B-Rep model for supporting recognition, classification, and retrieval, even transforming B-Rep model into high-level knowledge representation from low-level geometry descriptor [3].

B-Rep model is designed and stored in proprietary format in different CAD platform and transformed into a neutral STEP file for transferring, sharing, exchanging, and displaying in heterogeneous CAD environments. Under the guidance of STEP as an international standard, the different modeling methods result in almost the same STEP files. B-Rep model in STEP format is a hierarchy with geometric and topological elements of solid, shell, surface, loop, and edge.

Surfaces are as the key elements of B-Rep model in the paper. The view is attributed to the following facts. Firstly, surfaces are the nodes in AAG which is commonly used to express the topological and geometrical information of B-Rep model completely, and the type of large surface has the geometric even functional semantics. Secondly, surfaces are the primary factors of 3D objects from a psychological point of view. 3D shapes are spatial configurations of surface fragments encoded by IT neurons [4]. Gibson thought that the composition and layout of surfaces constitute what the values and meanings of things in the environment afford [5]. Gestalt psychologists try to settle how local discontinuities

in motion or depth are evaluated with respect to object boundaries and surfaces, and it hints that surfaces are the enhanced and ultimate cognitive elements of objects [6]. Marr regarded surface geometry as 3D shape representation [7]. Thirdly, people usually know complicated objects according to the systematology method; that is, an object is decomposed into parts and the similar parts are grouped together, and B-Rep model is naturally decomposed into surfaces; however mesh model is recognized either by the overall appearance or by artificially segmented patches.

Each surface of B-Rep model includes an interior region and one boundary bounded with curves. STEP describes surfaces with the four types of polygon plane, conic, swept, and b-spline. In the paper, surfaces were extracted from the neutral STEP file of B-Rep model, the curvatures of surface boundary and region were decomposed by wavelet transform method, and then the coefficient statistics of the same scale were as the surface feature vector. Similar surfaces of B-Rep model were clustered as a bin with the sum of perimeters and the mean vector; all bins constituting a histogram are finally as the feature vector of B-Rep model; thus B-Rep models are compared and retrieved using the EMD of histogram.

The rest of the paper is organized as follows. The related literature is discussed in Section 2. The coefficient statistics of same scale in wavelet transform were computed as the surface feature vector in Section 3. The similar surfaces of B-Rep model were clustered as a bin, and all bins are as the feature of B-Rep model in Section 4. The retrieval experiment of B-Rep models in NDR was finished and the result was discussed in Section 5. Conclusions and suggested future research were proposed in Section 6.

2. Related Works

There have been many shape feature modeling methods related to 3D CAD model in content-based 3D model retrieval field and with 3D object in computer vision field. But these shape feature recognition methods mainly refer to the visual appearance of 3D model rather than the particularity of B-Rep model. We can see these methods from three aspects.

Reference [8] alluded that titillating evidences from neuroscience indicate an elegant solution to 3D object recognition, thus providing the necessary motivation for radical rethinking of the computer vision strategies. It described the overviews of object recognition from the passive approaches and the active approaches. The geometric feature detection in the passive approaches was implemented using volumetric parts such as generalized cylinders, views of an object, Gestalt view and affordance view of perceptual organization, geometric invariants, shape-based components from images forming the aspect hierarchy, appearances represented by parametric eigenspace besides color and texture, local features, medial axis or skeleton, Fourier descriptors, edge direction histograms, and matching templates. The geometric feature detection in the active approaches was implemented using aspect graph by camera or eye movements, containing depth information.

In the current content-based 3D model retrieval field, the feature recognition approaches are mainly directed against

triangular mesh format of multimedia and visualization models, which reflects only external display properties rather than the internal structure relations, which are called the routine approaches for the general field. The feature recognition methods of B-Rep model currently adopt the routine approaches on condition that B-Rep model is first transformed into mesh format. The routine approaches are divided into three categories based on shape distribution, topology, and projection or view. Currently, photographic images are widely accessible due to the development of computer graphics hardware and 3D technologies, and methods based on views play an increasingly important role and people are more likely to divide 3D retrieval methods into two basic categories, model-based and view-based [9]. Shape distribution based methods set up the shape descriptors of the geometrical features or elements, for example, surface curvatures, vertices, and the distance between two random points [10]. Twelve different shape descriptors are proposed in the mechanical engineering domain [11]. Topology based methods involve how shape components are linked together, such as Reeb-Graphs, skeletons, and feature graphs [12–14], which are strongly related to the structure of the graph and hence to the topology of 3D models. View-based methods project 3D model into 2D line drawing images and extract the 2D image features to compare [15, 16]; the methods have currently provided effective and efficient retrieval results in many practical applications in which 3D models cannot be obtained [9], and the reference established a retrieval framework by clustering a free set of views captured from any direction without camera constraint [17].

Simple and complex features exist in the above both fields. The low-level shape features include corner points, edges, outlines, and medial axes. The high-level shape features include solid primitives, generalized cylinders, superquadrics, and other surfaces. However the above shape feature recognition approaches mainly for the appearance of 3D mesh model are not suitable for B-Rep model and the approaches on feature recognition fully considering the particularity of B-Rep model are mentioned in the following references. The hierarchical partition graph for B-Rep model retrieval is built by extracting winged-edge data structure [1]. An ontology-based feature recognition framework is proposed, in which the features are detected from STEP files and then represented as abstract concepts regarding some geometrical or topological patterns in order to share a common understanding of feature representation [18]. An approach to global and local reflective symmetry features for B-Rep model is proposed, which divides and conquers over AAG with the five types of faces as atomic entities [19]. It is often seen that manufacturing features are extracted by attributed adjacency subgraph matching from STEP files, for example, the various strings of cylinder and cross holes as the features of turned components [20]. The model signature graph (MSG) is mapped from AAG, and some B-Rep models are clustered according to the invariant topology vector of MSG such as vertex count, edge count, node degree, graph diameter, surface type counts, and edge type counts [21]. A complicated B-Rep model is represent as AAG from its STEP file, and its feature is recognized by matching the

AAG of simple B-Rep model annotated manually [3]. In model simplification to assure necessary shape information in collaborative product development and protect sensitive information on intellectual property, B-Rep model is usually simplified by directly keeping the key features and eliminating unnecessary features with smaller area ratio [22].

Wavelet transform reflects the characteristics of the frequency domain and the scale domain, whose coefficients are actually the degree of similarity of the shape and the given wavelet. Wavelet transform has been used for image compression and edge detection, also for shape similarity evaluation to match and recognize [23].

In above researches, the characteristics of surface as a kind of crucial shape descriptor are not described in detail, and the computation complexity for feature comparison of AAG graph matching is a NP-hard problem. Therefore, we propose the approach of shape feature recognition of B-Rep model based on surface wavelet transform to solve such problems.

3. Surface Features Based on Wavelet Transform

The key elements of a surface are its outer boundary and its region, so its features are recognized by analyzing its region with concavity and convexity as well as its boundary composed of lines and curves. Corner points reflect the crucial features of a surface boundary, and the Gauss points reveal the important features of a surface region, so the features are represented using wavelet transform.

3.1. Boundary Features by Wavelet Transform. The boundary of any surface type is closed by connected curves. Seen from the probabilistic graphical construction method [24], a graphics can be quickly and easily recognized by the polygon of corner points in its contour. Curvature distribution reflects well the actual situation of corner points; thus boundary curvatures are decomposed into boundary features using one-dimension wavelet transform method.

Boundary is considered with a vector variable in three-dimensional spatial-domain R^3 : $f(t) = \vec{C}(x(t), y(t), z(t))$, which is closed by parameter curve 0, 1, 2, ..., T-1: $f(t) = f_0(t_0) \cup f_1(t_1) \cup f_2(t_2) \cup \dots \cup f_{T-1}(t_{T-1})$, $0 \leq t_0, t_1 - 1, \dots \leq 1$.

The discrete curvature set of the boundary $f(t)$ is $fc = [fc_i], i = 1, 2, \dots, n$.

Its wavelet coefficient is the inner product between the curvature set fc and a wavelet function $\psi_{j,k}$:

$$c(j, k) = \langle fc, \psi_{j,k} \rangle = \int fc(t) \psi_{j,k}(t) dt \quad (1)$$

where j is a frequency scale and k is a location variable in frequency domain.

The coefficients of same scale j are analyzed statistically for translation and rotation invariant. Now the surface boundary feature vector is defined:

$$bfv = [S_k(c(j, k)), V_k(c(j, k))], \quad j = 1 \dots J \quad (2)$$

where S_k denotes the sum and V_k denotes the variance of coefficients on the same scale.

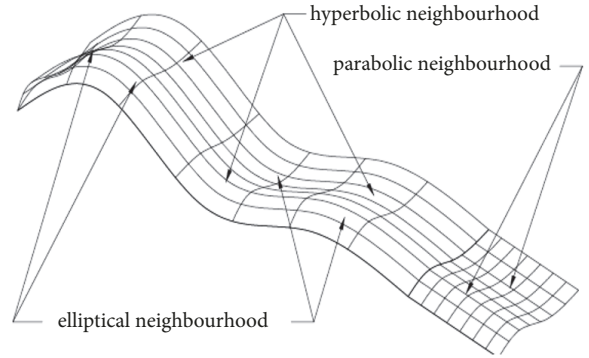


FIGURE 1: Gauss point in surface region.

3.2. Region Features by Wavelet Transform. Given the maximum principle curvature $k_1(u, v)$ and the minimum principle curvature $k_2(u, v)$ at point (u, v) on surface region $f(u, v) = \vec{S}(x(u, v), y(u, v), z(u, v))$, its Gauss curvature is $K(u, v) = k_1(u, v)k_2(u, v)$. The type of point (u, v) is, respectively, elliptical point, parabolic point, hyperbolic point according to $K > 0, K = 0(k_2 = 0), K < 0$, and all these points are called Gauss points, seen in Figure 1. In particular, if $k_1 = k_2 = 0$, the type of point (u, v) is planar point.

The distribution of Gauss point well reflects surface region characteristics; thus region curvatures are decomposed into region features by two-dimension wavelet transform method. Discrete curvature set of region $f(u, v)$ is $ru = [ru_{i,l}], i = 1, 2, \dots, n; l = 1, 2, \dots, m$.

Its wavelet coefficient is the inner product of curvature set ru and wavelet function ψ_{j,k_u,k_v} :

$$\begin{aligned} rc(j, k_u, k_v) &= \langle ru(u, v), \psi_{j,k_u,k_v} \rangle \\ &= \int ru(u, v) \psi_{j,k_u,k_v}(u, v) du dv \end{aligned} \quad (3)$$

where j is a frequency scale and k_u, k_v are location variables in frequency domain.

The coefficients of same scale j are analyzed statistically for translation and rotation invariant. Now the surface region feature vector is defined:

$$\begin{aligned} rfv &= [S_{k_u,k_v}(rc(j, k_u, k_v)), V_{k_u,k_v}(rc(j, k_u, k_v))], \\ &\quad j = 1, 2, \dots, J \end{aligned} \quad (4)$$

where S_{k_u,k_v} denotes the sum and V_{k_u,k_v} denotes the variance of coefficients on the same scale.

3.3. Surface Feature Vector. Surface perimeter and its edge number reflect whether it is important in B-Rep model. A larger surface is easier to arouse people's visual attention. A surface with a larger number of edges means more adjacent surfaces, and it more affects other surfaces. So surface perimeter sp and its edge number em are also regarded as other features.

Therefore surface feature vector is defined:

$$\begin{aligned} sfv = [sf_i] &= [sp, em, S_k(c(j, k)), V_k(c(j, k)), \\ &S'_{k_u, k_v}(rc(j, k_u, k_v)), V'_{k_u, k_v}(rc(j, k_u, k_v))] , \\ &j = 1, 2, \dots J \end{aligned} \quad (5)$$

4. Feature Recognition of B-Rep Model

4.1. Surface Histogram of B-Rep Model. B-Rep model is a closed shell surrounded by many surfaces, and it is usually represented as attributed surface adjacency graph (AAG). Among the surfaces of B-Rep model, larger surfaces with larger area or perimeter contribute to more remarkable visual shape features, and so do the surfaces with larger degree in AAG. Moreover, the similar surfaces generally reflect the common visual shape features and semantics. In fact, it is inspired by the human way of thinking; that is, people usually decompose complicated objects into parts and then compare them by every group of similar parts.

Thus B-Rep model or its AAG can be converted into a dendrogram or tree by clustering algorithm according to the Euclidean distance of surface features; hence the dendrogram is defined as the feature tree of B-Rep model. The father nodes of larger surfaces in the tree are selected as the feature bins of B-Rep model in order to simplify the calculation. The feature bins comprise a non-fixed-length unordered set, called surface histogram.

First, surface feature vector is normalized by $sf'_i = (sf_i - sf_{min}) / (sf_{max} - sf_{min})$; thus, the normalized feature vector is

$$\begin{aligned} sfv' &= [sp', em', S'_k(c(j, k)), V'_k(c(j, k)), \\ &S'_{k_u, k_v}(rc(j, k_u, k_v)), V'_{k_u, k_v}(rc(j, k_u, k_v))] \end{aligned} \quad (6)$$

Second, all surfaces of B-Rep model are clustered and transformed as the feature tree $FT = [t_l]$, and each node in the tree is a surface class with two parameters: average A_l and sum S_l of all members of the class:

$$FT = [t_l] = [(A_l([sf'_i]), S_l([sf'_i]))] \quad (7)$$

Third, the larger surfaces are extracted to characterize B-Rep model:

$$\begin{aligned} kt_s &= [sp', em', S'_k(c(j, k)), V'_k(c(j, k)), \\ &S'_{k_u, k_v}(rc(j, k_u, k_v)), V'_{k_u, k_v}(rc(j, k_u, k_v))] , \\ &sp' \geq c_1 \text{ && } em' \geq c_2 \end{aligned} \quad (8)$$

where c_1, c_2 are the thresholds of perimeter and edge number.

The surface histogram represents the feature of B-Rep model:

$$KF = [ktf_s] = [(A_s([sf'_i]), S_s([sf'_i]))] \quad (9)$$

where ktf_s is the father node of kt_s .

A typical B-Rep model is shown in Figure 2, and its feature tree and surface histogram are shown in Figure 3.

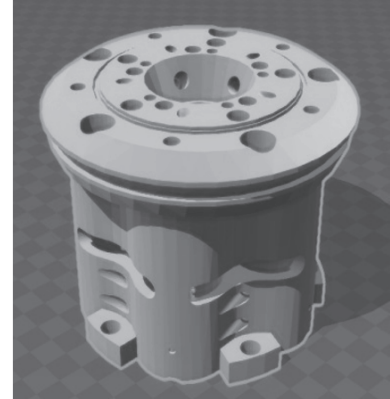


FIGURE 2: Torpedo B-Rep model.

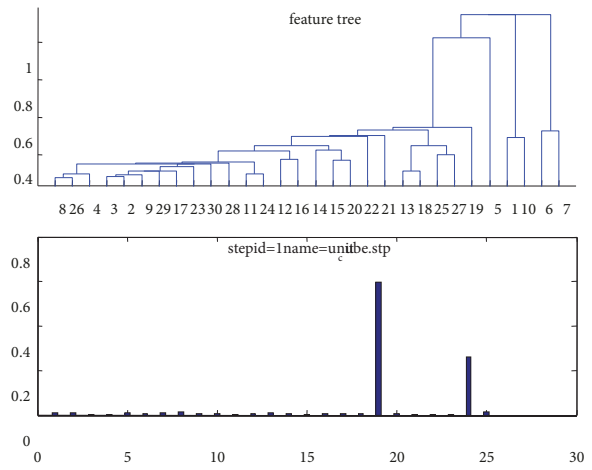


FIGURE 3: Feature tree and surface histogram.

4.2. Distance Measure of Both B-Rep Models. We need construct a metric space over the dataset of B-Rep models for computing their similarity, classification, and retrieval. A metric space is a collection of objects with a distance function $\delta(x, y)$, which computes the distance between any two elements in the set. Retrieval, clustering, and classification techniques make use of metric distance functions to organize and examine statistical distributions of data.

Three kinds of distance measure can be constructed, respectively, over the space of AAG, of feature tree, and of surface histogram.

Given two graphs G and H, graph edit distance is defined as the operation cost to transform G into H. It is well known that the distance computation is graph isomorphic mapping algorithm, and the problem is NP-complete, so there is no known algorithm for solving this problem in polynomial time, and even small instance set may require long computation time. It was also proven that the problem does not have an approximation algorithm running in polynomial time. So it is difficult directly to compare AAG of both B-Rep models.

We can compare two feature trees of B-Rep model using tree edit distance. Given two trees G and H, tree edit distance

is defined as the operation cost to transform G into H. The complexity of tree isomorphic mapping algorithm is $O(n^4)$ in the worst case [25].

We can compare both surface histograms of B-Rep model using earth mover's distance (EMD), and its complexity is $O(n^2)$ in the worst case. Moreover, the number n here is very smaller than in tree edit distance.

Although tree edit distance provides a proven metric for B-Rep model similarity, the cost of running the algorithm is much too high for a dataset that consists of thousands of B-Rep models. We make use of the relatively easy distance metric in a practical clustering and retrieval system. We believe that EMD metric among the feature bins of a surface histogram as an approximate solution will be suitable for clustering of B-Rep model dataset and for performing similarity-based queries.

Given both B-Rep models G and H, their feature bins of surface histogram are

$$GFB = [gf_s] = \left[\left(A_s ([sf'_i]), S_s (S_i (sf'_i)) \right) \right], \quad (10)$$

$$s = 1, 2, \dots, S$$

$$HFB = [hf_t] = \left[\left(A_t ([sf'_i]), S_t (S_i (sf'_i)) \right) \right], \quad (11)$$

$$t = 1, 2, \dots, T$$

The distance matrix of feature bins of B-Rep models is

$$D = [d_{st}] = \left[ND \left(A_s ([sf'_i]), A_t ([sf'_i]) \right) \right] \quad (12)$$

where ND is the normalized Euclidean distance.

The flow matrix of feature bins of B-Rep models is

$$FW = [f_{st}] = [fw(gf_s, hf_t)] \quad (13)$$

where fw is the flow of two bins.

So EMD ED of two B-Rep models is

$$ED_{G,H} = \min \left(\sum_{s=1}^S \sum_{t=1}^T d_{st} f_{st} \right) \quad (14)$$

which satisfies the following constraints:

$$\begin{aligned} f_{st} &\geq 0; \\ \sum_{s=1}^S f_{st} &\leq S_s (S_i (sf'_i)); \\ \sum_{t=1}^T f_{st} &\leq S_t (S_i (sf'_i)); \\ \sum_{s=1}^S \sum_{t=1}^T f_{st} &= \min \left(\sum_{s=1}^S S_s (S_i (sf'_i)), \sum_{t=1}^T S_t (S_i (sf'_i)) \right) \end{aligned} \quad (15)$$

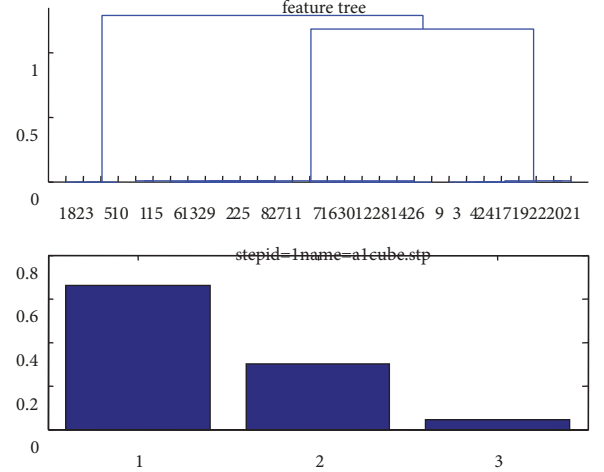


FIGURE 4: Cube dendrogram and histogram.

5. Experiment and Discussion

5.1. Retrieval Method. Since the goal of this paper is to recognize the features of B-Rep model, now retrieval methods are chosen to illustrate feasibility, and run-time and high quality are not issues at this point. The suitable similarity comparison and retrieval methods chosen correspond to EMD metric. The algorithms seek to use less EMD distance such that an object is more similar to the other objects.

Using the classification of a benchmark, we can define a measure of precision-recall for a particular model. The similarity comparison and retrieval algorithm are presented below in greater detail.

- (1) m histogram vectors (number-variable bins) are generated for m B-Rep models.
- (2) Randomly select a vector v_j from any class, and compute EMD between the other vectors and it.
- (3) Order by distance and calculate the precision value and recall value in the different retrieved numbers.
- (4) Repeat steps (2) and (3) to obtain the precision-recall curve of each type of B-Rep model in a benchmark.

5.2. Experimental Result Discussion in NDR. In the following experiments, the retrieval result of our algorithm is examined using the original classification in National Design Repository (NDR) as a benchmark. This dataset consists of 538 B-Rep 3D models, which are divided into 19 classes from regular cube to complex practical solid.

Firstly, regular-shape B-Rep models which are elementary models such as cube and cylinder from the primitives in NDR are tested. It is easy to check whether our method is consistent with human intuition using daily simple shapes. From the tests in which the same type of elementary models is feature modeled, the surface histogram is similar, and the bins in the histogram of a B-Rep model are corresponding to the surface types in the model one by one when the inconsistent threshold $cutoff$ is a certain value. For example, the results of the cube models with rounded corners are shown at $cutoff = 0.7$ in Figure 4, which contain plane, cylindrical surface, and

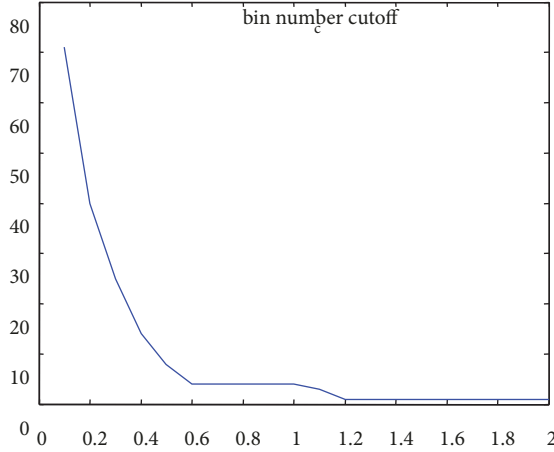


FIGURE 5: Consistent threshold and bin number.

TABLE 1: EMD variances of the elementary models.

	Cube	Cylinder	Sphere	Torus	Var. Sum
Intra-bin mean	10.7	19.6	28.1	11.1	16.6
Intra-bin variance	4.03	9.21	1.57	4.05	1868
Number	101	141	29	29	300
Between-bin variance	34.8	9	132.3	30.3	9499
Random Error			1868/(300-4)=6.3		
System error			9499/(4-1)=3166.3		
F			F=3166.3/6.3=502.6>3.78		

spherical surface. In addition, the bin number decreases as *cutoff* increases, shown in Figure 5. It proves that the shape feature recognition method according to surface types is a special case of our method.

While feature modeling on the elementary models in NDR, each bin of a histogram is set up on the basis of the inconsistent coefficient of Gaussian Distribution, and the intra-bin variances and the between-bin variances meet Hypothesis Testing *F* in Table 1; hence the bins can represent the principal components of B-Rep model.

It is important to perform a more detailed and refined distance comparison in response to a query. Objective distance tests for solid models are hard to define, so we used a more subjective testing methodology. We complete the retrieval tests according to EMD distance and the classification in NDR, the results shown in Table 2 and the precision-recall curves in Figure 6. Figure 6 shows that the shape comparison and retrieval algorithm are efficient to most classes in NDR.

Torpedo Motor from cast-then-machined in NDR, shown in Figure 2, is the complex and the unique model researchers particularly focused on, and Figure 7 tells us what models are more similar to it and how closely they look to each other visually.

For elementary models, the distance metric and the retrieval method are no doubt accurate. The metric accuracy

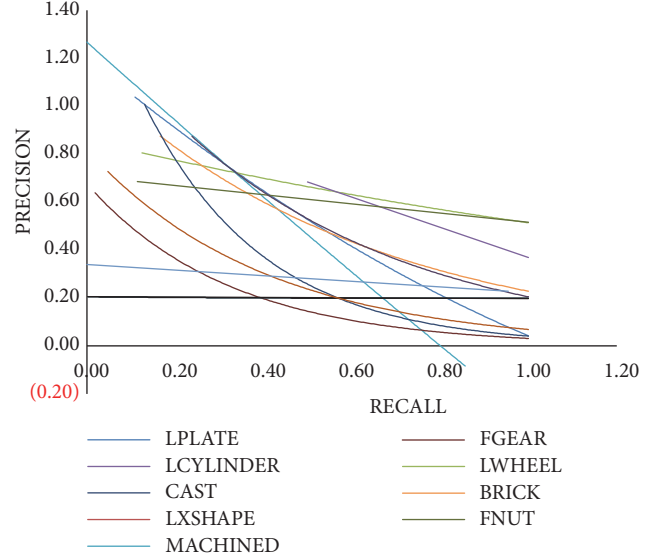


FIGURE 6: Precision-recall in NDR.

for more complex shapes is acceptable and consistent with human vision since finding a similar complex model is a daunting task to do manually.

6. Conclusion and Future Works

In the paper, B-Rep model is presented as surface based features by deconstructing its STEP files, and the properties of each surface are extracted with wavelet transform. The current methods of shape feature recognition and comparison for mesh models get the overall appearance characteristics and 2.5D information. Some seek to segment mesh models and label each part to understand, and it is heading in the same direction with our method for B-Rep model. Most surfaces of B-Rep model have semantics and functions, and it is the normal cognitive process to segment, classify, and group according to surface elements. However it is rare to compare B-Rep format files to recognize 3D models in the industrial product field and the computer vision field; now our method to recognize the shape features of B-Rep model is much meaningful.

There are still some problems to be solved: the parameters in the surface wavelet transform can be adjusted well through the use of large-scale data; the STEP shape benchmark needs to be extended in order to check algorithm effectiveness and efficiency.

Data Availability

The data used to support the findings of this study are available from the corresponding author upon request.

Conflicts of Interest

The author declares that there are no conflicts of interest regarding the publication of this paper.

TABLE 2: Part of the retrieval result of each classification.

		P	R		P	R
3706.hh.stp	3706.hh.stp			4019.hh.stp	4019.hh.stp	
LXSHAPE	LXSHAPE	0.14	1	LWHEEL	LWHEEL	0.25
LXSHAPE	LXSHAPE	0.29	1	LWHEEL	LWHEEL	0.5
LXSHAPE	LXSHAPE	0.43	1	LWHEEL	LWHEEL	0.75
LXSHAPE	LXSHAPE	0.57	1	LWHEEL	FBOLT	
LXSHAPE	LXSHAPE	0.71	1	LWHEEL	CUBE	
LXSHAPE	LXSHAPE	0.86	1	LWHEEL	CUBE	
LXSHAPE	LXSHAPE	1	1	LWHEEL	MACHINED	
LXSHAPE	PCYLINDER			LWHEEL	CUBE	

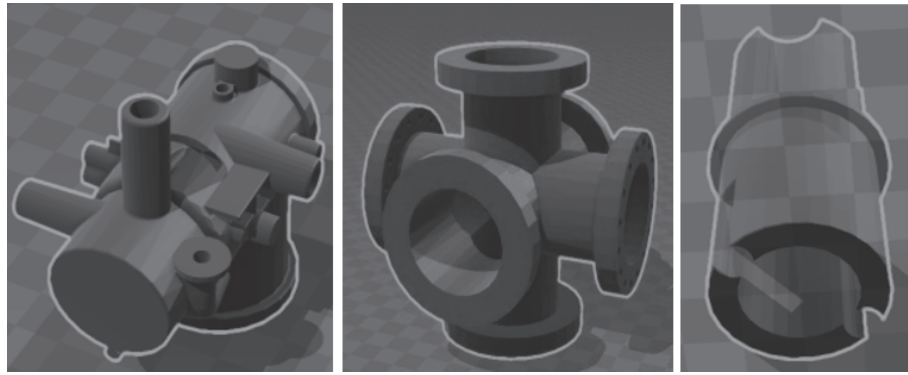


FIGURE 7: Similar models to Torpedo.

Acknowledgments

This work was supported by The National Natural Science Foundation of China (61472233), The Natural Science Foundation of Shandong Province (ZR2014FM018), and Shandong Provincial Key Laboratory for Distributed Computer Software Novel Technology.

References

- [1] Z. Li, X. Zhou, and W. Liu, “A geometric reasoning approach to hierarchical representation for B-rep model retrieval,” *Computer-Aided Design*, vol. 62, pp. 190–202, 2015.
- [2] S. Jayanti, Y. Kalyanaraman, and K. Ramani, “Shape-based clustering for 3D CAD objects: A comparative study of effectiveness,” *Computer-Aided Design*, vol. 41, no. 12, pp. 999–1007, 2009.
- [3] Z. Wang, L. Tian, and W. Duan, “Annotation and retrieval system of CAD models based on functional semantics,” *Chinese Journal of Mechanical Engineering*, vol. 27, no. 6, pp. 1112–1124, 2014.
- [4] Y. Yamane, E. T. Carlson, K. C. Bowman, Z. Wang, and C. E. Connor, “A neural code for three-dimensional object shape in macaque inferotemporal cortex,” *Nature Neuroscience*, vol. 11, no. 11, pp. 1352–1360, 2008.
- [5] J. J. Gibson, “An ecological approach to visual perception,” *American Journal of Psychology*, vol. 102, no. 4, pp. 443–76, 1979.
- [6] I. Kovács, “Gestalten of today: Early processing of visual contours and surfaces,” *Behavioural Brain Research*, vol. 82, no. 1, pp. 1–11, 1996.
- [7] H. Barlow, “Vision: A computational investigation into the human representation and processing of visual information,” *Journal of Mathematical Psychology*, vol. 27, no. 1, pp. 107–110, 1983.
- [8] A. Andreopoulos and J. K. Tsotsos, “50 Years of object recognition: directions forward,” *Computer Vision and Image Understanding*, vol. 117, no. 8, pp. 827–891, 2013.
- [9] Y. Gao and Q. Dai, “View-based 3D object retrieval: challenges and approaches,” *IEEE MultiMedia*, vol. 21, no. 3, pp. 52–57, 2014.
- [10] R. Osada, T. Funkhouser, B. Chazelle, and D. Dobkin, “Shape distributions,” *ACM Transactions on Graphics*, vol. 21, no. 4, pp. 807–832, 2002.
- [11] S. Jayanti, Y. Kalyanaraman, N. Iyer, and K. Ramani, “Developing an engineering shape benchmark for CAD models,” *Computer-Aided Design*, vol. 38, no. 9, pp. 939–953, 2006.
- [12] N. D. Cornea, *Curve-Skeletons: Properties, Computation and Applications*, Rutgers University New Brunswick, New Brunswick, NJ, USA, 2007.
- [13] V. Cicirello and W. C. Regli, “Machining feature-based comparisons of mechanical parts,” in *Proceedings of the 2001 International Conference on Shape Modeling and Applications, SMI 2001*, pp. 176–184, May 2001.
- [14] A. Elinson, D. S. Nau, and W. C. Regli, “Feature-based Similarity Assessment of Solid Models,” in *Proceedings of the Fourth ACM/SIGGRAPH Symposium on Solid Modeling & Applications Atlanta*, pp. 297–310, 2010.
- [15] M. Eitz, R. Richter, T. Boubekeur, K. Hildebrand, and M. Alexa, “Sketch-based 3D shape retrieval,” *ACM Transactions on Graphics*, 2010.

- [16] T. Furuya and R. Ohbuchi, "Ranking on cross-domain manifold for sketch-based 3D model retrieval," in *Proceedings of the 2013 International Conference on Cyberworlds, CW 2013*, pp. 274–281, October 2013.
- [17] Y. Gao, J. Tang, R. Hong et al., "Camera constraint-free view-based 3-D object retrieval," *IEEE Transactions on Image Processing*, vol. 21, no. 4, pp. 2269–2281, 2012.
- [18] Q. Wang and X. Yu, "Ontology based automatic feature recognition framework," *Computers in Industry*, vol. 65, no. 7, pp. 1041–1052, 2014.
- [19] K. Li, G. Foucault, J.-C. Léon, and M. Trlin, "Fast global and partial reflective symmetry analyses using boundary surfaces of mechanical components," *Computer-Aided Design*, vol. 53, pp. 70–89, 2014.
- [20] V. N. Malleswari, P. M. Valli, and M. M. M. Sarcar, "Automatic Recognition of Machining Features using STEP Files," *International Journal of Engineering Research & Technology*, vol. 2, no. 3, 2013.
- [21] B. M. Peabody and W. C. Regli, *Clustering Technique for Databases of CAD Models*, 2010.
- [22] R. Sun, S. Gao, and W. Zhao, "Technical Section: An approach to B-rep model simplification based on region suppression," *Computers & Graphics*, vol. 34, no. 5, pp. 556–564, 2010.
- [23] X. Qi. Shape Matching, "Using Wavelet Transform Modulus," in *Proceedings of the International Conference on Computer Sciences*, pp. 389–393, Honolulu, Hawaii, 2004.
- [24] F. Attneave, "Some informational aspects of visual perception," *Psychological Review*, vol. 61, no. 3, pp. 183–193, 1954.
- [25] J. Wang, H. Liu, and H. Wang, "A mapping-based tree similarity algorithm and its application to ontology alignment," *Knowledge-Based Systems*, vol. 56, pp. 97–107, 2014.

